Eur. Phys. J. B (2019) 92: 53
https://doi.org/10.1140/epjb/e2019-90656-2

THE EUROPEAN PHYSICAL JOURNAL B

Regular Article

# Electrostatic chameleons: theory of intelligent metashells with adaptive response to inside objects

Liujun Xu and Jiping Huang[a]

Department of Physics, State Key Laboratory of Surface Physics, and Key Laboratory of Micro and Nano Photonic Structures (MOE), Fudan University, Shanghai 200433, P.R. China

Received 7 November 2018 / Received in final form 12 January 2019
Published online 4 March 2019


**Abstract.** The remarkable capability to tailor material property has largely expanded the permittivity range, even with negative value. However, permittivity, as an inherent property, may lack adaptive response to nearby objects. To solve this problem, here we introduce the chameleon behavior from biology to electrostatics. The essence of electrostatic chameleons can be concluded as intelligent metashells with adaptive response to inside objects. The requirement of electrostatic chameleons is deduced by making the effective permittivities of metashells only dependent on the permittivities of inside objects. By delicately designing the anisotropic permittivities of metashells, we summarize two types of electrostatic chameleons with distinct mechanisms. The theoretical analyses are validated by numerical simulations, which indicate that the proposed metashells do work as expected. Such schemes have potential applications in camouflage, self-adaption, etc. This work not only lays the theoretical foundation for electrostatic chameleons, but also provides guidance for exploring other intelligent materials beyond chameleon.

## 1 Introduction

The range of material parameters has been largely expanded with artificial structures, such as negative permittivity [1], negative permeability [2], negative refraction index [3–7], etc. However, these inherent parameters, once designed, may lack the adaptive response to nearby objects.

Recently, intellectualization has become one of the research focuses of material science for the potential applications in optical and microwave devices, such as coding metasurface [8,9], chameleonlike cloak [10], light-operated device [11,12], invisible sensor [13,14], etc. Therefore, it is urgent to solve the fundamental problem for realizing intelligent parameters like permittivity.

Inspired by the natural phenomenon that chameleons can adaptively change their color according to their nearby environment, we expect to introduce this phenomenon from biology to electrostatics. In other words, electrostatic chameleons can adaptively change their permittivities according to their nearby objects.

For this purpose, we study the electrostatic properties of a fundamental core-shell structure which has been widely explored [15–28]. Researches have found that by adjusting geometry, anisotropy, and constituents of core-shell structures, many unique properties can be realized, such as partial resonance [15,16], nonlinear enhancement [17–19], surface plasmon resonance [20–23], etc.

However, comparing with the previous researches on core-shell structures, we first calculate the effective permittivities of anisotropic shells when the components of diagonal tensors are abnormal ($\varepsilon_{\theta\theta}/\varepsilon_{rr} < 0$ for two dimensions, and $\varepsilon_{\theta\theta}/\varepsilon_{rr} < -1/8$ for three dimensions). With the delicate design of tensorial permittivities, shells can exhibit adaptive response to inside cores, and always possess the same permittivities as those of inside cores, thus they are called as intelligent metashells, or chameleon metashells.

## 2 Theory of electrostatic chameleons

We start from considering the effective permittivities of electrostatic chameleons, for the key point focuses on the adaptive permittivities. We consider the two-dimensional (2D) system shown in Figure 1a, which is separated into three regions. They are object (region I), chameleon metashell (region II), and background (region III). The tensorial permittivities of object, chameleon metashell, and background are respectively $\overleftrightarrow{\varepsilon}_1^{2D}$, $\overleftrightarrow{\varepsilon}_2^{2D}$, and $\overleftrightarrow{\varepsilon}_3^{2D}$. We suppose that the object and background are isotropic, and the chameleon metashell is anisotropic: $\overleftrightarrow{\varepsilon}_1^{2D} = \varepsilon_1 \overleftrightarrow{I}_2$, $\overleftrightarrow{\varepsilon}_3^{2D} = \varepsilon_3 \overleftrightarrow{I}_2$, and $\overleftrightarrow{\varepsilon}_2^{2D} = \mathrm{diag}\,(\varepsilon_{rr}, \varepsilon_{\theta\theta})$, where $\overleftrightarrow{I}_2$ is the second-order identity tensor. The parameters

[a] e-mail: jphuang@fudan.edu.cn

are expressed in cylindrical coordinates $(r, \theta)$. We can derive the effective permittivity of region I+II (denoted by $\varepsilon_e^{2D}$) as

$$\varepsilon_{e>}^{2D} = m_1\varepsilon_{rr}\frac{\varepsilon_1 + m_1\varepsilon_{rr} + (\varepsilon_1 - m_1\varepsilon_{rr})\left(\sqrt{p_{2D}}\right)^{2m_1}}{\varepsilon_1 + m_1\varepsilon_{rr} - (\varepsilon_1 - m_1\varepsilon_{rr})\left(\sqrt{p_{2D}}\right)^{2m_1}}, \tag{1}$$

$$\varepsilon_{e<}^{2D} = n\varepsilon_{rr}\frac{\varepsilon_1 + n\varepsilon_{rr}\tan\left(n\ln\sqrt{p_{2D}}\right)}{n\varepsilon_{rr} - \varepsilon_1\tan\left(n\ln\sqrt{p_{2D}}\right)}, \tag{2}$$

where $\varepsilon_{e>}^{2D}$ ($\varepsilon_{e<}^{2D}$) is for $\varepsilon_{\theta\theta}/\varepsilon_{rr} > 0$ ($\varepsilon_{\theta\theta}/\varepsilon_{rr} < 0$). $m_1 = \sqrt{\varepsilon_{\theta\theta}/\varepsilon_{rr}}$, $n = \sqrt{-\varepsilon_{\theta\theta}/\varepsilon_{rr}}$, and $p_{2D} = (r_1/r_2)^2$ is the area fraction. Detailed derivation can be found in Part I of Appendix A.

We calculate $\varepsilon_e^{2D}$ when $\varepsilon_{\theta\theta}/\varepsilon_{rr}$ respectively approaches $0^+$ and $0^-$, and find that they tend to the same value,

$$\varepsilon_{e=}^{2D} = \varepsilon_{rr}\frac{\varepsilon_1 - \varepsilon_{\theta\theta}\ln\sqrt{p_{2D}}}{\varepsilon_{rr} - \varepsilon_1\ln\sqrt{p_{2D}}}, \tag{3}$$

where $\varepsilon_{e=}^{2D}$ is for $\varepsilon_{\theta\theta}/\varepsilon_{rr} = 0$.

As the name suggests, electrostatic chameleons should adaptively change their effective permittivities (denoted as $\varepsilon_2$) according to inside object, which can be mathematically expressed as

$$\varepsilon_2 = \varepsilon_1. \tag{4}$$

Since the effective permittivity of region I or II is $\varepsilon_1$, that of region I + II has the only possibility to be

$$\varepsilon_e^{2D} = \varepsilon_1. \tag{5}$$

Comparing equation (5) with equations (3) and (2), we can obtain the requirement of electrostatic chameleons as

$$\varepsilon_{\theta\theta}/\varepsilon_{rr} \approx 0: \ \varepsilon_{\theta\theta} \approx 0 \text{ with } \varepsilon_{rr} \gg \varepsilon_1, \tag{6}$$

$$\varepsilon_{\theta\theta}/\varepsilon_{rr} < 0: \ \sqrt{-\varepsilon_{\theta\theta}/\varepsilon_{rr}}\ln\sqrt{p_{2D}} = -Z^+\pi, \tag{7}$$

where $Z^+ (= 1, 2, 3, \ldots)$ is positive integers. Clearly, equations (6) and (7) respectively make equations (3) and (2) satisfy the requirement of equation (5).

Then we explore the electrostatic chameleons in three-dimensional (3D) system shown in Figure 1d. Similarly, the tensorial permittivities of object (regions I), chameleon metashell (region II), and background (region III) are respectively $\overleftrightarrow{\varepsilon}_1^{3D}$, $\overleftrightarrow{\varepsilon}_2^{3D}$, and $\overleftrightarrow{\varepsilon}_3^{3D}$. We suppose that the object and background are isotropic, and the chameleon metashell is anisotropic: $\overleftrightarrow{\varepsilon}_1^{3D} = \varepsilon_1\overleftrightarrow{I}_3$, $\overleftrightarrow{\varepsilon}_3^{3D} = \varepsilon_3\overleftrightarrow{I}_3$, $\overleftrightarrow{\varepsilon}_2^{3D} = \mathrm{diag}(\varepsilon_{rr}, \varepsilon_{\theta\theta}, \varepsilon_{\varphi\varphi})$, where $\overleftrightarrow{I}_3$ is the third-order identity tensor. The parameters are written in spherical coordinates $(r, \theta, \varphi)$. We suppose $\varepsilon_{\theta\theta} = \varepsilon_{\varphi\varphi}$ for simplicity, and derive the effective permittivity of region I + II (denoted as $\varepsilon_e^{3D}$),

$$\varepsilon_{e>}^{3D} = \varepsilon_{rr}\frac{u_1(\varepsilon_1 - \varepsilon_{rr}u_2) - u_2(\varepsilon_1 - \varepsilon_{rr}u_1)\left(\sqrt[3]{p_{3D}}\right)^{u_1-u_2}}{(\varepsilon_1 - \varepsilon_{rr}u_2) - (\varepsilon_1 - \varepsilon_{rr}u_1)\left(\sqrt[3]{p_{3D}}\right)^{u_1-u_2}}, \tag{8}$$

$$\varepsilon_{e<}^{3D} = \varepsilon_{rr}\frac{4\varepsilon_1 v + \left[2\varepsilon_1 + \left(1 + 4v^2\right)\varepsilon_{rr}\right]\tan\left(v\ln\sqrt[3]{p_{3D}}\right)}{4\varepsilon_{rr}v - 2(2\varepsilon_1 + \varepsilon_{rr})\tan\left(v\ln\sqrt[3]{p_{3D}}\right)}, \tag{9}$$

where $\varepsilon_{e>}^{3D}$ ($\varepsilon_{e<}^{3D}$) is for $\varepsilon_{\theta\theta}/\varepsilon_{rr} > -1/8$ ($\varepsilon_{\theta\theta}/\varepsilon_{rr} < -1/8$). $u_{1,2} = \left(-1 \pm \sqrt{1 + 8\varepsilon_{\theta\theta}/\varepsilon_{rr}}\right)/2$, $v = \sqrt{-1 - 8\varepsilon_{\theta\theta}/\varepsilon_{rr}}/2$, and $p_{3D} = (r_1/r_2)^3$ is the volume fraction. Detailed calculations can be found in Part II of Appendix A.

We calculate $\varepsilon_e^{3D}$ when $\varepsilon_{\theta\theta}/\varepsilon_{rr}$ approaches $-1/8^+$ and $-1/8^-$, and they also tend to the same value,

$$\varepsilon_{e=}^{3D} = \varepsilon_{rr}\frac{4\varepsilon_1 + (2\varepsilon_1 + \varepsilon_{rr})\ln\sqrt[3]{p_{3D}}}{4\varepsilon_{rr} - 2(2\varepsilon_1 + \varepsilon_{rr})\ln\sqrt[3]{p_{3D}}}, \tag{10}$$

where $\varepsilon_{e=}^{3D}$ is for $\varepsilon_{\theta\theta}/\varepsilon_{rr} = -1/8$.

We resort to equations (10) and (9) to realize electrostatic chameleons in three dimensions. For this realization, equation (9) works, but equation (10) fails. Nevertheless, we find a pseudo electrostatic chameleon when $\varepsilon_{\theta\theta}/\varepsilon_{rr} = 0$, whose effective permittivity is

$$\varepsilon_e^{3D} = \varepsilon_{rr}\frac{\varepsilon_1\sqrt[3]{p_{3D}}}{\varepsilon_{rr} + \varepsilon_1\left(1 - \sqrt[3]{p_{3D}}\right)}, \tag{11}$$

which is similar to the condition in two dimensions, namely equation (3).

This can then be concluded as

$$\varepsilon_{\theta\theta}/\varepsilon_{rr} \approx 0: \varepsilon_{rr} \gg \varepsilon_1, \tag{12}$$

$$\varepsilon_{\theta\theta}/\varepsilon_{rr} < -1/8: \left(\sqrt{-1 - 8\varepsilon_{\theta\theta}/\varepsilon_{rr}}/2\right)\ln\sqrt[3]{p_{3D}} = -Z^+\pi, \tag{13}$$

where $Z^+ (= 1, 2, 3, \ldots)$ is positive integers.

Equations (12) and (13) respectively make equations (11) and (9) become $\varepsilon_e^{3D} = \sqrt[3]{p_{3D}}\varepsilon_1$ and $\varepsilon_e^{3D} = \varepsilon_1$, which is distinctly different from two dimensions. In other words, equation (12) only works as a pseudo electrostatic chameleon due to the extra constant $\sqrt[3]{p_{3D}}$.

So far, we may give a classification of electrostatic chameleons. We define "type A" electrostatic chameleons as those with $\varepsilon_{\theta\theta}/\varepsilon_{rr} \approx 0$, and here 0 is just a constant, which is equal to the demarcation point in two dimensions by accident. And we define "type B" electrostatic chameleons as those with $\varepsilon_{\theta\theta}/\kappa_{rr}$ smaller than the demarcation point ($\varepsilon_{\theta\theta}/\varepsilon_{rr} < 0$ for 2D and $\varepsilon_{\theta\theta}/\varepsilon_{rr} < -1/8$ for 3D). We can then conclude that there are two types (type A and type B) of electrostatic chameleons in two dimensions (Fig. 1b), and only one type (type B) of electrostatic chameleons in three dimensions (Fig. 1e). Nevertheless, there is a pseudo type A electrostatic chameleons (due to

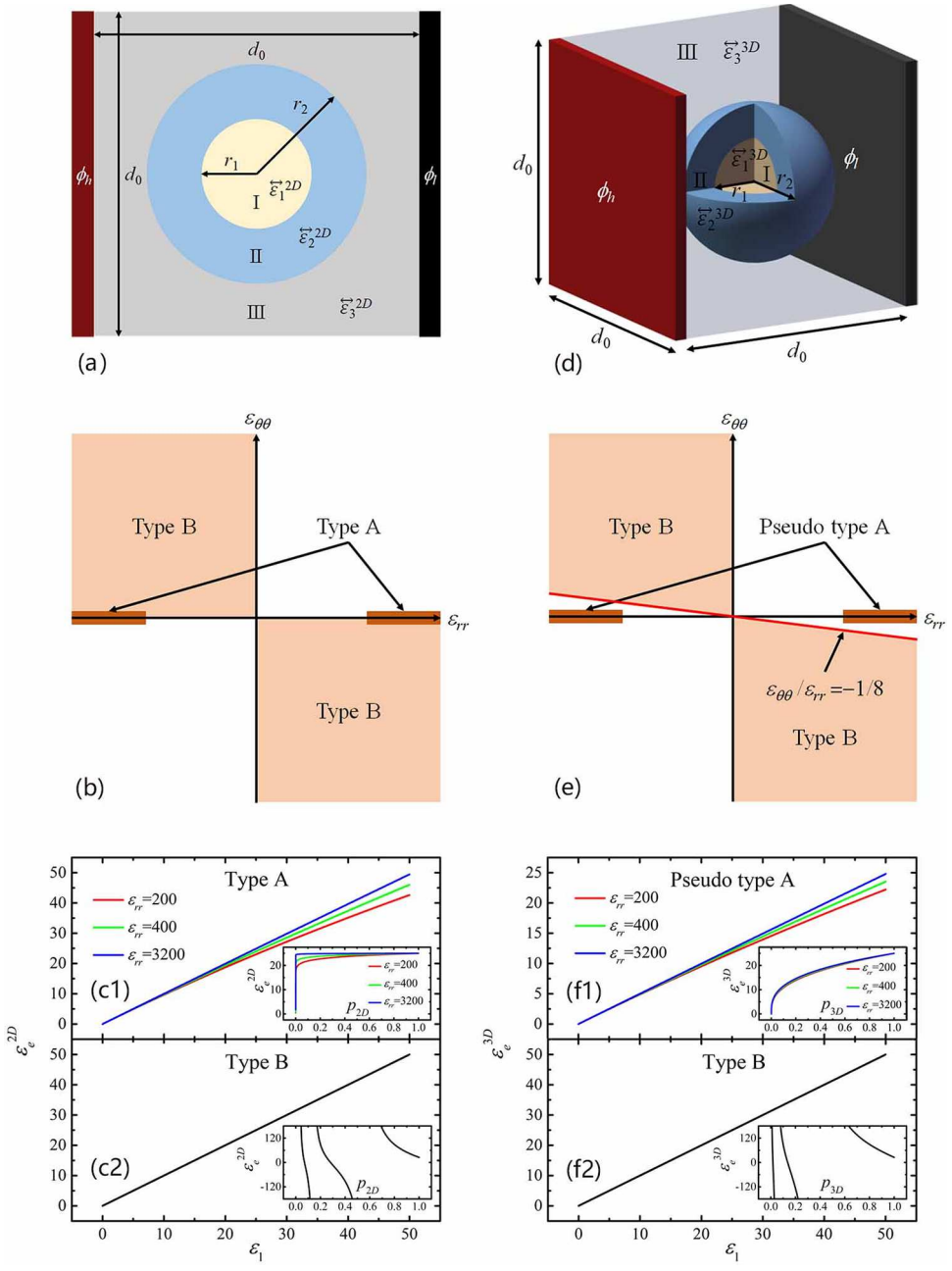


**Fig. 1.** Electrostatic chameleons for (a–c2) two dimensions and (d–f2) three dimensions. (a, d) are schematic diagrams, and (b, e) are classifications. (c1, c2, f1, f2) show the calculated effective permittivities $\varepsilon_e^{2D}$ (or $\varepsilon_e^{3D}$), as a function of $\varepsilon_1$. Concrete parameters: (c1) $\varepsilon_{\theta\theta} = 0.001$, $p = 0.25$; (c2) $\varepsilon_{rr} = -20$ and $Z^+ = 1$ in equation (7), $p = 0.25$; (f1) $\varepsilon_{\theta\theta} = 0.001$, $p = 0.125$; (f2) $\varepsilon_{rr} = -40$ and $Z^+ = 1$ in equation (13), $p = 0.125$. The insets of (c1, c2, f1, f2) show the calculated effective permittivities $\varepsilon_e^{2D}$ (or $\varepsilon_e^{3D}$), as a function of $p_{2D}$ (or $p_{3D}$), where $\varepsilon_1 = 25$ and the corresponding chameleon metashells are kept unchanged.

the extra constant $\sqrt[3]{p_{3D}}$) in three dimensions (Fig. 1e). Therefore, type A electrostatic chameleons are related to the dimension, but type B electrostatic chameleons are general (namely, independent of the dimension). Moreover, type A electrostatic chameleons result from an approximate solution (Fig. 1c1; bigger $\varepsilon_{rr}$ is better), and the phenomenon is almost independent of area fraction excluding extremely small value (inset of Fig. 1c1). The pseudo type A electrostatic chameleons also result from an approximate solution (Fig. 1f1; bigger $\varepsilon_{rr}$ is better), but the phenomenon is dependent on volume fraction (inset of Fig. 1f1). Differently, type B electrostatic chameleons originate from an exact solution (Figs. 1c2 and 1f2), but the phenomena are dependent on core fraction, especially featured by the quasi-periodic variations with core fraction (insets of Figs. 1c2 and 1f2). Therefore, the two types (type A and type B) of chameleons possess distinct mechanisms despite of the similar chameleon behavior. To be mentioned, the highly anisotropic parameters of type A electrostatic chameleons are similar to those in

magnetostatics for realizing long-distance transfer [29] or three-dimensional magnetic cloak [30].

## 3 Simulation of electrostatic chameleons

To validate the theory, we perform finite-element simulations based on the commercial software COMSOL Multiphysics (http://www.comsol.com/).

### 3.1 Two-dimensional electrostatic chameleons

We first discuss the type A electrostatic chameleons. The simulation box of Figures 2a–2f is separated into three regions just like Figure 1a. Chameleon metashells, normal shells, and comparative shells are respectively applied in region II of Figures 2a, 2d; 2b, 2e; and 2c, 2f. The parameters of chameleon metashells echo with the blue line in Figure 1c1. We observe the electric profile of background (region III) to check whether the effective permittivity of the metashell (region II) changes with the inside object (region I). For the convenience of comparison, we set the background (region III) to have the same permittivity as the corresponding object (region I).

When the designed chameleon metashell reaches an object (Fig. 2a), it can adaptively change its effective permittivity according to inside object, which results in the same electric profile in the background (region III) as the comparative shell (Fig. 2c). However, the normal shell distorts the background equipotential lines (Fig. 2b) due to its different permittivity. We then change the permittivity of the object, but keep the metashell unchanged (Fig. 2d). As a result, the effective permittivity of the chameleon metashell also adaptively changes, which results in the same background equipotential lines as the comparative shell (Fig. 2f). In this case, the normal shell fails to change again (Fig. 2e).

We further extend the type A electrostatic chameleons from three aspects: from uniform to non-uniform electric fields, from isotropic to anisotropic objects, and from circular to arbitrary shapes. Chameleon metashells, normal shells, and comparative shells are also respectively applied in Figures 3a, 3d, 3g; 3b, 3e, 3h; and 3c, 3f, 3i. The same background electric fields between Figures 3a, 3c (3d, 3f or 3g, 3i) show that the chameleon metashells are robust under more complicated conditions. However, the different background electric fields between Figures 3b, 3c (3e, 3f or 3h, 3i) show that the normal shells fail to change their permittivities accordingly.

We then discuss the type B electrostatic chameleons. For brevity, we replace type A chameleon metashells in Figures 2a, 2d and Figures 3a, 3d with type B chameleon metashells, and keep the other parameters unchanged. The parameters of chameleon metashells echo with the black line in Figure 1c2. The same background electric fields between Figure 4a and Figure 2c (Fig. 4b and Fig. 2f, Fig. 4c and Fig. 3c, Fig. 4d and Fig. 3f) validate the type B chameleon metashells. To be mentioned, the type B chameleons are not suitable for non-circular shapes.

After considering the anisotropic objects in both type A and type B electrostatic chameleons, equation (4) can thus

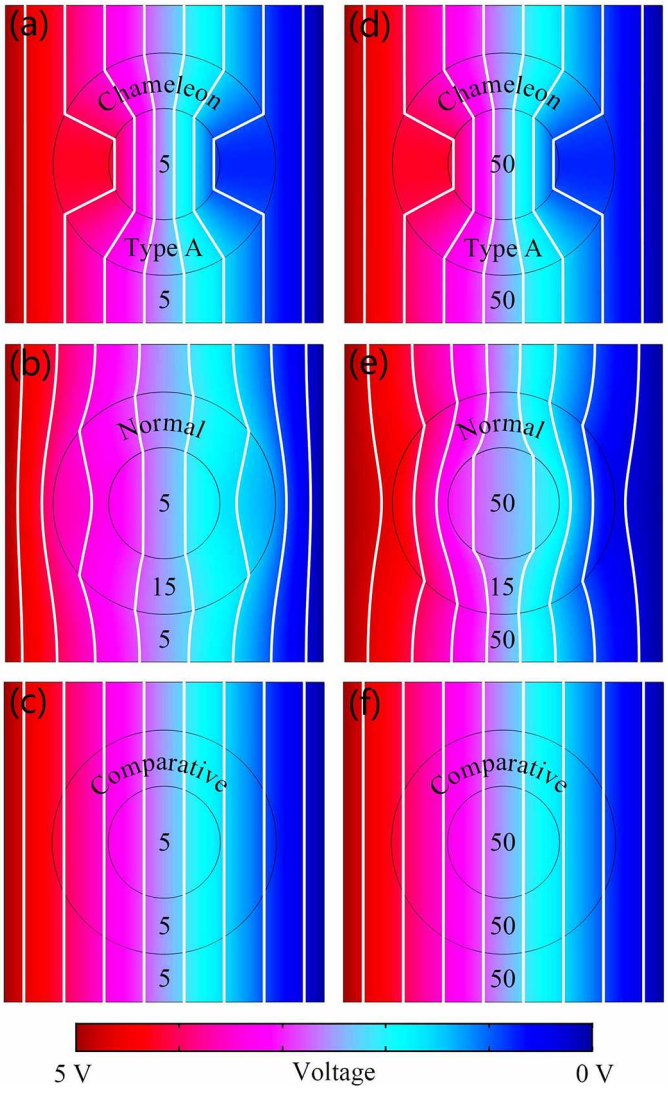


**Fig. 2.** Simulations of two-dimensional type A electrostatic chameleons. White lines represent equipotential lines. The permittivities of (a, d) chameleon metashells and (b, e) normal shells are respectively diag (3200, 0.001) (in cylindrical coordinate) and 15. The permittivities of object (Region I) and background (Region III) are set to be the same, which are respectively (a, b, c) 5 and (d, e, f) 50. The permittivities of comparative shells in (c, f) are the same as those of the corresponding objects. Other parameters: $d_0 = 20\,\text{cm}$; $r_1 = 3.5\,\text{cm}$; and $r_2 = 7\,\text{cm}$.

be extended as

$$\overleftrightarrow{\varepsilon}_2 = \overleftrightarrow{\varepsilon}_1, \tag{14}$$

under the requirement of equation (6) or (7).

### 3.2 Three-dimensional electrostatic chameleons

We discuss the pseudo type A electrostatic chameleons. Similarly, chameleon metashells, normal shells, and comparative shells are applied in Figures 5a, 5d; 5b, 5e; and 5c, 5f, respectively. For pseudo type A electrostatic

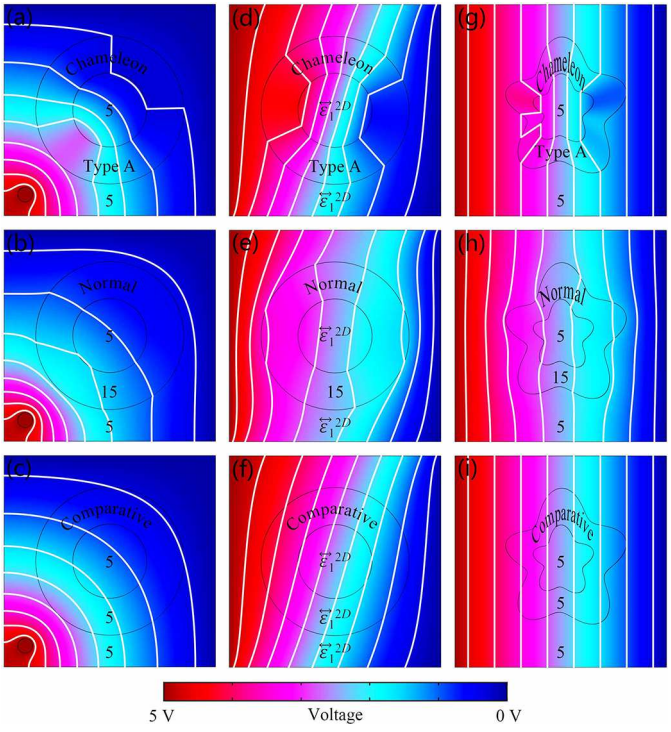


**Fig. 3.** Extensions of two-dimensional type A electrostatic chameleons. (a–c) Non-uniform electric fields generated by point electric sources; (d–f) anisotropic objects; and (g–i) arbitrary shapes. The permittivities of object/background are (a–c, g–i) 5 and (d–f) [(3, 2), (2, 5)] (in Cartesian coordinates). The comparative shells in (c, f, i) have the same permittivities as the corresponding objects. Other parameters are the same as those for Figure 2.

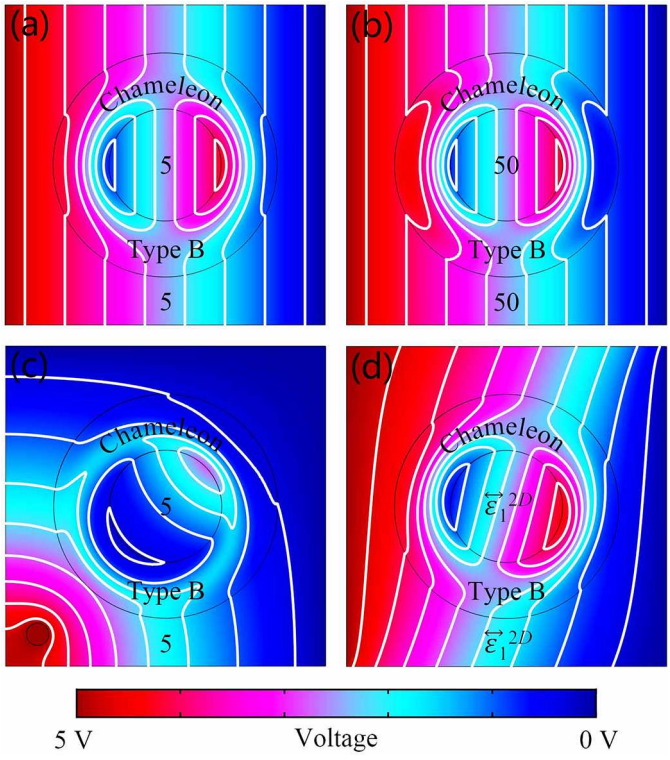


**Fig. 4.** Simulations of two-dimensional type B electrostatic chameleons. The chameleon metashells in (a–d) are $\varepsilon_{rr} = -20$ and $Z^+ = 1$ in equation (7). The other parameters of (a, b, c, d) are respectively the same as those of Figure 2a, Figure 2d, Figure 3a, and Figure 3d.

chameleons are not real chameleons (due to the extra constant $\sqrt[3]{p_{3D}}$), here we set the background to have $\sqrt[3]{p_{3D}}\,(= 0.5)$ times of permittivity as the corresponding objects, except Figures 5c, 5f. The parameters of chameleon metashells echo with the blue line in Figure 1f1. The same background electric fields between Figures 5a, 5c (or Figs. 5d, 5f) validate the adaptive permittivities of the pseudo type A chameleon metashells. However, the different background electric fields between Figures 5b, 5c (or Figs. 5e, 5f) show that normal shells fail to change their permittivities.

We extend the pseudo type A electrostatic chameleons from three aspects: from uniform to non-uniform electric fields, from isotropic to anisotropic objects, and from circular to non-circular shapes. Chameleon metashells, normal shells, and comparative shells are respectively applied in Figures 6a, 6d, 6g; 6b, 6e, 6h; and 6c, 6f, 6i. The same background electric fields between Figures 6a, 6c (6d, 6f or 6g, 6i) show that the pseudo type A chameleon metashells are robust under more realistic conditions. However, the different background electric fields between Figures 6b, 6c (6e, 6f or 6h, 6i) show that the normal shells fail to change their permittivities accordingly. To be mentioned, the pseudo type A chameleons are suitable for non-circular shapes, but not for arbitrary shapes especially when the inner and outer boundaries of the chameleon metashells are different.

Then we discuss the type B electrostatic chameleons. The parameters of chameleon metashells echo with the black line in Figure 1f2. For brevity, we replace pseudo type A chameleon metashells in Figures 5a, 5d and Figures 6a, 6d with type B chameleon metashells. For type B electrostatic chameleons are real chameleons, here we set the background to have the same permittivity as the corresponding object. The same background electric fields between Figure 7a and Figure 5c (Fig. 7b and Fig. 5f, Fig. 7c and Fig. 6c, or Fig. 7d and Fig. 6f) validate the type B chameleon metashells. To be mentioned, type B electrostatic chameleons are not suitable for non-circular shapes.

After considering the anisotropic object in both pseudo type A and type B electrostatic chameleons, equation (4) can thus be extended as

$$\overleftrightarrow{\varepsilon}_2 = \sqrt[3]{p_{3D}}\,\overleftrightarrow{\varepsilon}_1, \tag{15}$$

$$\overleftrightarrow{\varepsilon}_2 = \overleftrightarrow{\varepsilon}_1, \tag{16}$$

under the requirement of equation (12) or (13).

## 4 Discussion and conclusion

It is worth noting that negative permittivities are required for fabricating type B chameleon metashells. For this realization, we can refer to negative permeabilities in

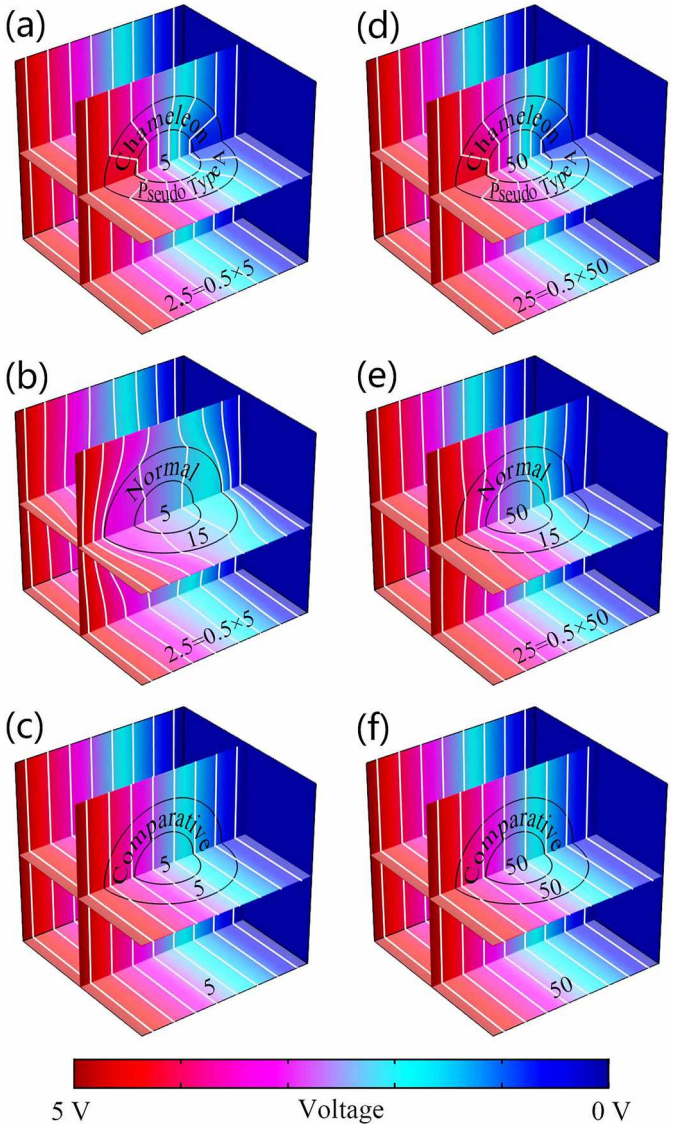


**Fig. 5.** Simulations of three-dimensional pseudo type A electrostatic chameleons. The permittivities of (a, d) chameleon metashells and (b, e) normal shells are respectively diag (3200, 0.001, 0.001) (in cylindrical coordinate) and 15. The permittivities of background (Region III) are $\sqrt[3]{p_{3D}}$ (= 0.5) times of those of object (Region I), except (c, f), which are respectively (a–c) 5 and (d–f) 50 for objects. The permittivities of comparative shells and background in (c, f) are the same as those of the corresponding objects. Other parameters: $d_0 = 20\,\text{cm}$; $r_1 = 3.5\,\text{cm}$; and $r_2 = 7\,\text{cm}$.

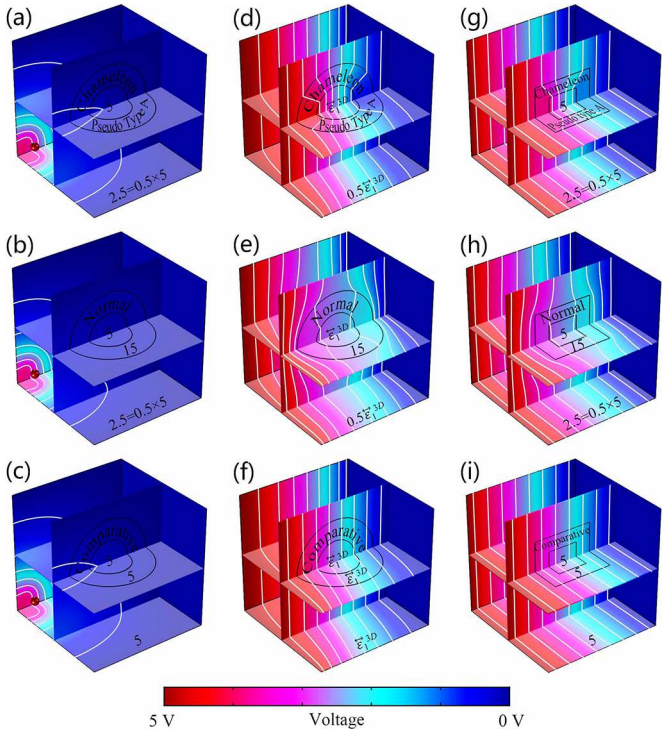


**Fig. 6.** Extensions of three-dimensional pseudo type A electrostatic chameleons. (a–c) non-uniform electric fields generated by point electric sources; (d–f) anisotropic objects; and (g–i) non-circular shapes (5×5×5 and 10×10×10 cm for inner and outer boundaries of the cubic chameleon metashell). The permittivities of background (Region III) are $\sqrt[3]{p_{3D}}$ (= 0.5) times of those of object (Region I), except (c, f, i), which are respectively (a–c, g–i) 5 and (d–f) [(3, 2, 0), (2, 5, 0), (0, 0, 5)] (in Cartesian coordinates) for objects. The permittivities of comparative shells and background in (c, f, i) are the same as those of the corresponding objects. Other parameters are the same as those for Figure 5.

magnetostatics realized by adding external current [31]. Similarly, negative permittivities can also be achieved by adding external stimuli appropriately. In other words, the type B chameleon metashells require active materials (with external stimuli), whereas type A chameleon metashells only require passive materials (without external stimuli). From this point, type A chameleon metashells (passive material with adaptive response) may be more counterintuitive than type B chameleon metashells (active material with adaptive response).

Moreover, this work may reveal some clues for unique properties of low-dimensional materials in macroscopic scale. Generally speaking, functional devices can be naturally extended from two dimensions to three dimension with some changes of parameters and structures, such as negative refraction index [5,7]. However, it is different when discussing type A chameleon metashells which cannot be directly extended to three dimensions. Such results may provide clues for studying low-dimensional transportation in macroscopic scale.

This work also first derives the effective permittivity under the demarcation point ($\varepsilon_{\theta\theta}/\varepsilon_{rr} < 0$ for 2D and $\varepsilon_{\theta\theta}/\varepsilon_{rr} < -1/8$ for 3D). Especially, the quasi-periodic variation with core fraction (insets of Figs. 1c2, 1f2) is first revealed in this work, which are dramatically different from the well-known effective medium theories like the Maxwell-Garnett formula [32] and the Bruggeman formula [33].

In summary, the electrostatic chameleons proposed in this work can work adaptively for different inside objects. Such chameleon metashells have potential applications in camouflage, self-adaptivity, etc. This work also offers

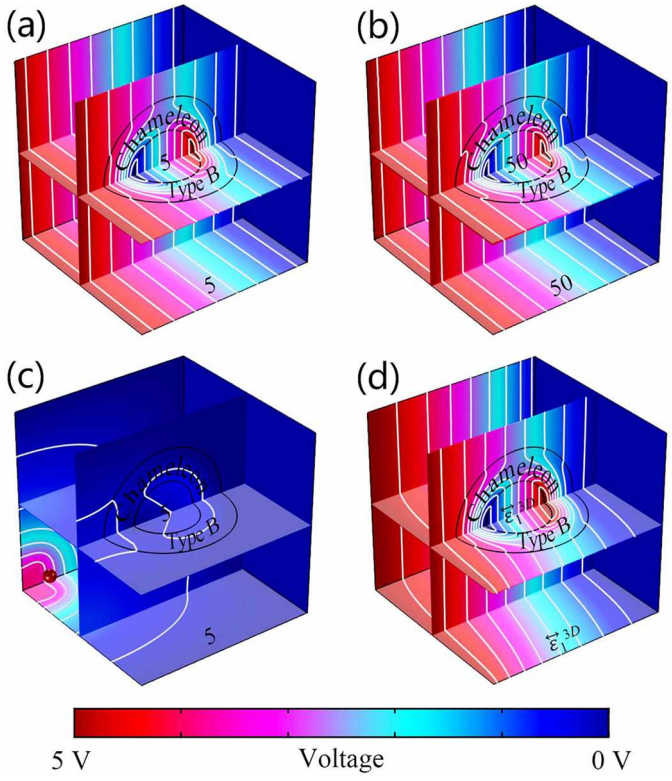


**Fig. 7.** Simulations of three-dimensional type B electrostatic chameleons. The chameleon metashells in (a–d) are $\varepsilon_{rr} = -40$ and $Z^+ = 1$ in equation (13). The other parameters of (a, b, c, d) are respectively the same as those of Figure 5a, Figure 5d, Figure 6a, and Figure 6d, except the permittivities of background, which are set to be the same as those of corresponding objects.

guidance for magnetostatic camouflage [31,34,35], and designing similar chameleon behavior in magnetostatics where permeabilities play the same role as permittivities in electrostatics. The chameleon behavior of permittivities and permeabilities may further contributes to the manipulation of electromagnetic wave, such as illusion [36].

We acknowledge the financial support by the National Natural Science Foundation of China under Grant No. 11725521, and by the Science and Technology Commission of Shanghai Municipality under Grant No. 16ZR1445100.

## Author contribution statement

Both the two authors were involved in the preparation of the manuscript. The two authors have read and approved the final manuscript. L.X. and J.H. designed research; L.X. performed research; L.X. and J.H. analyzed data; and L.X. and J.H. wrote the paper.

## Appendix A

### Part I: Theory for two dimensions

We consider the passive Gauss's law to derive the effective permittivity,

$$\boldsymbol{\nabla} \cdot \left(-\overleftrightarrow{\varepsilon}\boldsymbol{\nabla}\phi\right) = 0, \tag{A.1}$$

where $\overleftrightarrow{\varepsilon}$ and $\phi$ are respectively tensorial permittivity and electric potential.

In region II, equation (A.1) can be rewritten in cylindrical coordinates as

$$\frac{1}{r}\frac{\partial}{\partial r}\left(r\varepsilon_{rr}\frac{\partial\phi_2^{2D}}{\partial r}\right) + \frac{1}{r}\frac{\partial}{\partial\theta}\left(\varepsilon_{\theta\theta}\frac{\partial\phi_2^{2D}}{r\partial\theta}\right) = 0, \tag{A.2}$$

where $\phi_2^{2D}$ is the electric potential in region II. $\phi_1^{2D}$ and $\phi_3^{2D}$ are defined by analogy.

The general solution of equation (A.2) is

$$\begin{aligned}\phi_{2>}^{2D} = {} & A_{0>}^{2D} + B_{0>}^{2D}\ln r \\ & + \sum_{i=1}^{\infty}\left[A_{i>}^{2D}\sin(i\theta) + B_{i>}^{2D}\cos(i\theta)\right] r^{im_1} \\ & + \sum_{j=1}^{\infty}\left[C_{j>}^{2D}\sin(j\theta) + D_{j>}^{2D}\cos(j\theta)\right] r^{jm_2}, \end{aligned} \tag{A.3}$$

$$\begin{aligned}\phi_{2<}^{2D} = {} & A_{0<}^{2D} + B_{0<}^{2D}\ln r \\ & + \sum_{i=1}^{\infty}\left[A_{i<}^{2D}\sin(i\theta) + B_{i<}^{2D}\cos(i\theta)\right]\cos(in\ln r) \\ & + \sum_{j=1}^{\infty}\left[C_{j<}^{2D}\sin(j\theta) + D_{j<}^{2D}\cos(j\theta)\right]\sin(jn\ln r), \end{aligned} \tag{A.4}$$

where $\phi_{2>}^{2D}$ ($\phi_{2<}^{2D}$) is for $\varepsilon_{\theta\theta}/\varepsilon_{rr} > 0$ ($\varepsilon_{\theta\theta}/\varepsilon_{rr} < 0$). $m_{1,2} = \pm\sqrt{\varepsilon_{\theta\theta}/\varepsilon_{rr}}$, and $n = \sqrt{-\varepsilon_{\theta\theta}/\varepsilon_{rr}}$. Here $\varepsilon_{\theta\theta}/\varepsilon_{rr} = 0$ is the demarcation point.

The general solution in region I ($\phi_1^{2D}$) or III ($\phi_3^{2D}$) is the right side of equation (A.3) for $m_{1,2} = \pm 1$. As a result, we can obtain $\phi_3^{2D}$ as

$$\phi_3^{2D} = A_0^{2D} + B_1^{2D} r\cos\theta + D_1^{2D} r^{-1}\cos\theta. \tag{A.5}$$

The undetermined coefficients in $\phi_1^{2D}$, $\phi_2^{2D}$ and $\phi_3^{2D}$ can be determined by the following boundary conditions,

$$\begin{cases} \phi_1^{2D} < \infty, \\ \phi_1^{2D}(r_1) = \phi_2^{2D}(r_1), \\ \phi_2^{2D}(r_2) = \phi_3^{2D}(r_2), \\ \left(-\varepsilon_1\partial\phi_1^{2D}/\partial r\right)_{r_1} = \left(-\varepsilon_{rr}\partial\phi_2^{2D}/\partial r\right)_{r_1}, \\ \left(-\varepsilon_{rr}\partial\phi_2^{2D}/\partial r\right)_{r_2} = \left(-\varepsilon_3\partial\phi_3^{2D}/\partial r\right)_{r_2}, \\ \boldsymbol{\nabla}\phi_3^{2D}(r\to\infty) = \boldsymbol{\nabla}\phi_0, \end{cases} \tag{A.6}$$

where $\nabla\phi_0$ represents the external uniform electric gradient.

By setting $D_1^{2D}$ of $\phi_3^{2D}$ as zero to ensure the background electric field undistorted, we can derive the effective permittivity of region I + II (denoted by $\varepsilon_e^{2D}$) as equations (1) and (2).

### Part II: Theory for three dimensions

Compared with two dimensions, electrostatic chameleons in three dimensions possess different properties. Considering the axial symmetry $\varepsilon_{\theta\theta} = \varepsilon_{\varphi\varphi}$, $\phi$ is independent of $\varphi$.

In region II, equation (A.1) can be rewritten in spherical coordinates as

$$\frac{1}{r^2}\frac{\partial}{\partial r}\left(r^2\varepsilon_{rr}\frac{\partial\phi_2^{3D}}{\partial r}\right)+\frac{1}{r\sin\theta}\frac{\partial}{\partial\theta}\left(\sin\theta\varepsilon_{\theta\theta}\frac{\partial\phi_2^{3D}}{r\partial\theta}\right)=0, \tag{A.7}$$

where $\phi_2^{3D}$ is the electric potential in region II. $\phi_1^{3D}$ and $\phi_3^{3D}$ are defined by analogy.

The general solution of equation (A.7) is

$$\begin{aligned}\phi_{2\geq}^{3D} &= A_{0\geq}^{3D}+B_{0\geq}^{3D}r^{-1}\\ &\quad+\sum_{i=1}^{\infty}\left(A_{i\geq}^{3D}r^{s_1}+B_{i\geq}^{3D}r^{s_2}\right)P_i\left(\cos\theta\right), \qquad (A.8)\\ \phi_{2\sim}^{3D} &= A_{0\sim}^{3D}+B_{0\sim}^{3D}r^{-1}\\ &\quad+\sum_{i=1}^{j}\left(A_{i\sim}^{3D}r^{s_1}+B_{i\sim}^{3D}r^{s_2}\right)P_i\left(\cos\theta\right)\\ &\quad+\sum_{i=j+1}^{\infty}r^{-1/2}\left[A_{i\sim}^{3D}\cos(t\ln r)+B_{i\sim}^{3D}\sin(t\ln r)\right]\\ &\quad\times P_i\left(\cos\theta\right), \qquad (A.9)\\ \phi_{2<}^{3D} &= A_{0<}^{3D}+B_{0<}^{3D}r^{-1}\\ &\quad+\sum_{i=1}^{\infty}r^{-1/2}\left[A_{i<}^{3D}\cos(t\ln r)+B_{i<}^{3D}\sin(t\ln r)\right]\\ &\quad\times P_i\left(\cos\theta\right), \qquad (A.10)\end{aligned}$$

where $\phi_{2\geq}^{3D}$ is for $\varepsilon_{\theta\theta}/\varepsilon_{rr}\geq 0$, $\phi_{2\sim}^{3D}$ is for $0>\varepsilon_{\theta\theta}/\varepsilon_{rr}>-1/8$, and $\phi_{2<}^{3D}$ is for $\varepsilon_{\theta\theta}/\varepsilon_{rr}<-1/8$. The indexes of $s_{1,2}=\left(-1\pm\sqrt{1+4i\left(i+1\right)\varepsilon_{\theta\theta}/\varepsilon_{rr}}\right)/2$, the indexes of $t=\sqrt{-1-4i\left(i+1\right)\varepsilon_{\theta\theta}/\varepsilon_{rr}}/2$, and the index of $j=\mathrm{Int}\left[\left(-1+\sqrt{1-\varepsilon_{rr}/\varepsilon_{\theta\theta}}\right)/2\right]$, where $i$ is the summation index in equations (A.8)–(A.10), and $\mathrm{Int}\left[\cdots\right]$ is the integral function with respect to ... $P_i$ is Legendre polynomials. We also find that equations (A.8) and (A.9) are essentially the same under the similar boundary conditions equation (A.6), for we only care about the term of $i=1$. Therefore, $\varepsilon_{\theta\theta}/\varepsilon_{rr}=-1/8$ is the real demarcation point.

The general solution in region I ($\phi_1^{3D}$) or III ($\phi_3^{3D}$) is the right side of equation (A.8) for $s_1=1$ and $s_2=-2$. As a result, we can obtain $\phi_3^{3D}$ as

$$\phi_3^{3D}=A_0^{3D}+A_1^{3D}r\cos\theta+B_1^{3D}r^{-2}\cos\theta. \tag{A.11}$$

By setting $B_1^{3D}$ of $\phi_3^{3D}$ as zero to ensure the background electric field undistorted, we can derive the effective permittivity of region I + II (denoted by $\varepsilon_e^{3D}$) as equations (8) and (9).

## References


1. J.B. Pendry, A.J. Holden, W.J. Stewart, I. Youngs, Phys. Rev. Lett. **76**, 4773 (1996)
2. J.B. Pendry, A.J. Holden, D.J. Robbins, W.J. Stewart, IEEE Trans. Micro. Theory **47**, 2075 (1999)
3. D.R. Smith, N. Kroll, Phys. Rev. Lett. **85**, 2933 (2000)
4. J.B. Pendry, Phys. Rev. Lett. **85**, 3966 (2000)
5. R.A. Shelby, D.R. Smith, S. Schultz, Science **292**, 77 (2001)
6. J. Li, L. Zhou, C.T. Chan, P. Sheng, Phys. Rev. Lett. **90**, 083901 (2003)
7. J. Valentine, S. Zhang, T. Zentgraf, E.U. Avila, D.A. Genov, G. Bartal, X. Zhang, Nature **455**, 376 (2008)
8. L.H. Gao, Q. Cheng, J. Yang, S.J. Ma, J. Zhao, S. Liu, H.B. Chen, Q. He, W.X. Jiang, H.F. Ma, Q.Y. Wen, L.J. Liang, B.B. Jin, W.W. Liu, L. Zhou, J.Q. Yao, P.H. Wu, T.J. Cui, Light Sci. Appl. **4**, e324 (2015)
9. T.J. Cui, S. Liu, L.L. Li, Light Sci. Appl. **5**, e16172 (2016)
10. R.G. Peng, Z.Q. Xiao, Q. Zhao, F.L. Zhang, Y.G. Meng, B. Li, J. Zhou, Y.C. Fan, P. Zhang, N.H. Shen, T. Koschny, C.M. Soukoulis, Phys. Rev. X **7**, 011033 (2017)
11. W.X. Jiang, C.Y. Luo, S. Ge, C.W. Qiu, T.J. Cui, Adv. Mater. **27**, 4628 (2015)
12. T.C. Han, Y.X. Liu, L. Liu, J. Qin, Y. Li, J.Y. Bao, D.Y. Ni, C.W. Qiu, Sci. Rep. **8**, 12208 (2018)
13. T.Z. Yang, X. Bai, D.L. Gao, L.Z. Wu, B.W. Li, J.T.L. Thong, C.W. Qiu, Adv. Mater. **27**, 7752 (2015)
14. R. Mach-Batlle, C. Navau, A. Sancheza, Appl. Phys. Lett. **112**, 162406 (2018)
15. N.A. Nicorovici, R.C. Mcphedran, G.W. Milton, Phys. Rev. B **49**, 8479 (1994)
16. O. Levy, J. Appl. Phys. **77**, 1696 (1995)
17. P.M. Hui, C. Xu, D. Stroud, Phys. Rev. B **69**, 014203 (2004)
18. J.P. Huang, K.W. Yu, Phys. Rep. **431**, 87 (2006)
19. D.H. Liu, C. Xu, P.M. Hui, Appl. Phys. Lett. **92**, 181901 (2008)
20. S.Y. Park, D. Stroud, Appl. Phys. Lett. **85**, 2920 (2004)
21. S.Y. Park, D. Stroud, Phys. Rev. Lett. **94**, 217401 (2005)
22. A. Alu, N. Engheta, Phys. Rev. E **72**, 016623 (2005)
23. V. Levin, M. Markova, A. Mousatov, E. Kazatchenko, E. Pervago, Eur. Phys. J. B **90**, 192 (2017)
24. H.R. Ma, B.S. Zhang, W.Y. Tam, P. Sheng, Phys. Rev. B **61**, 962 (2000)
25. Y.L. Geng, X.B. Wu, L.W. Li, B.R. Guan, Phys. Rev. E **70**, 056609 (2004)
26. C.W. Qiu, L.W. Li, T.S. Yeo, S. Zouhdi, Phys. Rev. E **76**, 039903 (2007)

27. G.Q. Gu, E.B. Wei, Y.M. Poon, F.G. Shin, Phys. Rev. B **76**, 064203 (2007)
28. M. Cristea E.C. Niculescu, Eur. Phys. J. B **85**, 191 (2012)
29. C. Navau, J. Prat-Camps, O. Romero-Isart, J.I. Cirac, A. Sanchez, Phys. Rev. Lett. **112**, 253901 (2014)
30. J.F. Zhu, W. Jiang, Y.C. Liu, G. Yin, J. Yuan, S.L. He, Y.G. Ma, Nat. Commun. **6**, 8931 (2015)
31. R.M. Batlle, A. Parra, S. Laut, N.D. Valle, C. Navau, A. Sanchez, Phys. Rev. Appl. **9**, 034007 (2018)
32. J.C. Maxwell Garnett, Philos. Trans. R. Soc. London Ser. A **203**, 385 (1904)
33. D.A.G. Bruggeman, Ann. Phys. (Leipzig) **24**, 636 (1935)
34. F. Gomory, M. Solovyov, J. Souc, C. Navau, J.P. Camps, A. Sanchez, Science **335**, 1466 (2012)
35. W. Jiang, Y.G. Ma, S.L. He, Phys. Rev. Appl. **9**, 054041 (2018)
36. Y. Lai, J. Ng, H.Y. Chen, D.Z. Han, J.J. Xiao, Z.Q. Zhang, C.T. Chan, Phys. Rev. Lett. **102**, 253902 (2009)